Symmetry-Switching Molecular Fe(O-2)(n)(+) Clusters

ARTICLE *in* THE JOURNAL OF PHYSICAL CHEMISTRY A · JUNE 2011

Impact Factor: 2.69 · DOI: 10.1021/jp204478v · Source: PubMed

4 AUTHORS:

Giannis Mpourmpakis
University of Pittsburgh
61 PUBLICATIONS **1,214** CITATIONS
SEE PROFILE

Michalis Velegrakis
Foundation for Research and Technology - H…
41 PUBLICATIONS **425** CITATIONS
SEE PROFILE

Claudia Mihesan
Petru Poni Institute of Macromolecular Che…
20 PUBLICATIONS **218** CITATIONS
SEE PROFILE

Antonis Andriotis
Foundation for Research and Technology - H…
133 PUBLICATIONS **2,993** CITATIONS
SEE PROFILE

THE JOURNAL OF PHYSICAL CHEMISTRY A

ARTICLE

pubs.acs.org/JPCA

Symmetry-Switching Molecular $Fe(O_2)_n^+$ Clusters

Giannis Mpourmpakis, Michalis Velegrakis,* Claudia Mihesan, and Antonis N. Andriotis

Institute of Electronic Structure and Laser, FORTH, Heraklion 71110, Crete, Greece

Supporting Information

ABSTRACT: Experimental and theoretical studies based on mass spectrometry, collision-induced dissociation, and ab initio calculations are performed on the formation and stability of FeO_n^+ clusters, as well as on their structural, electronic, and magnetic properties. In the mass spectra, clusters with an even number of oxygen atoms show increased stability, most prominently for FeO_{10}^+. The extra stability of this cluster is confirmed by measurements of fragmentation cross sections through crossed molecular beam experiments. In addition, the calculations indicate a structural phase transition at this size, and most importantly, the FeO_n^+ clusters show unique magnetic features, exhibiting isoenergetic low-spin (LS) and high-spin (HS) ground states. In the LS state, the magnetic moments of the O atoms adopt an antiferromagnetic alignment with respect to the magnetic moment of Fe^+, whereas in the HS state, the alignment is ferromagnetic. FeO_{10}^+ is the largest thermodynamicaly stable complex, with the highest magnetic moment among the FeO_n^+ clusters (13 μ_B in HS).

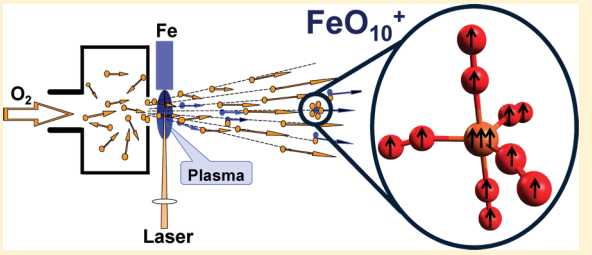

1. INTRODUCTION

In the course of understanding corrosion, biological and catalytic processes (e.g., CO oxidation) and in the search of new magnetic nanomaterials, much effort has been focused recently on iron oxide clusters (see, for example, ref 1 and references therein). Iron oxide clusters have been produced in the past in various laboratories.[2−10] In the majority of these studies, laser vaporization of a solid target in the presence of O_2 was employed to form mainly Fe_mO_n clusters with $m > 1$. However, iron forms a large number of complexes at various stoichiometries when it interacts with oxygen. A characteristic case is that of oxygen-rich FeO_n clusters. For these small complexes, only a few experimental[2,4,6,9,10] and theoretical studies[4,11−14] have been reported, investigating their formation and stability.

Only recently, Gutsev et al.[15] extended the theoretical studies of neutral and negative iron oxide clusters to larger sizes ($n \leq 12$). A common feature of the theoretical studies[1,4,11−15] is the use of density functional theory (DFT) in the spin-polarized generalized electron density gradient approximation (SGGA). As for other transition metal oxides, the study of Fe_mO_n clusters encounters the problems related to the drawback of the DFT/SGGA in describing incomplete d shells. The theoretical results appear to be sensitive to the approximations made in incorporating the electron correlations. For instance, even though the theoretical results[12] obtained for FeO_n, ($n \leq 4$, neutral and negative species) using molecular orbital theory at the BPW91 level of approximation are in good agreement with the experimental data, they deviate from the results obtained at the B3LYP level of approximation (hybrid-DFT). On the other hand, B3LYP reproduces accurately both experimental and theoretical results, obtained at a high level of theory, on Fe^+-containing compounds.[16]

In most of the Fe−O complexes studied, the oxygen is in the atomic state, directly bonded to the Fe atoms/ions. In a few cases, however, evidence of molecular O_2 bonding to the core of the complex was reported, such as, for example, in the FeO_5 system, where an O_2 molecule was considered as an adduct to the FeO_3 core.[11,14] In the theoretical study of Gutsev et al.[15] on FeO_n and FeO_n^- clusters ($n = 5−12$), the authors investigated a series of structural configurations and showed that the ground states of the clusters containing an even number of O atoms exhibit superoxo- and peroxo-type bonding, whereas the clusters with an odd number of O atoms include one or more oxo-type bondings.

In the present work, we report the experimental formation of gas-phase FeO_n^+, $n \leq 16$ clusters. Additionally, we measure fragmentation cross sections of cluster ions colliding with a Ne secondary beam, using the crossed molecular beam scattering method. Moreover, by using first-principle calculations, we reveal the appearance of approximately isoenergetic low- and high-spin states and a structural phase transition as the number of O ligands bonded to Fe^+ increases.

2. EXPERIMENTAL AND THEORETICAL METHODS

2.1. Experimental Setup. The experiments have been performed in a molecular beam apparatus described in detail previously.[17−20] In short, a beam of iron oxide clusters is formed in an open source without a growth channel by mixing the plasma plume produced by fundamental (1064 nm) or quadrupled (266 nm) Nd:YAG laser ablation of pure iron with the supersonic

Received: May 13, 2011
Revised: May 26, 2011
Published: May 26, 2011

expansion of molecular oxygen from a pulsed nozzle placed a few millimeters above the target. The formed cationic species are accelerated at laboratory energy of E_{Lab} = 1.5 keV and mass separated in a pulsed double-field time-of-flight (TOF) mass spectrometer equipped with a microchannel plate (MCP) detector. TOF spectra are recorded with a digital storage oscilloscope.

For measuring the fragmentation cross sections of the clusters, a secondary beam of Ne atoms is crossed perpendicularly in the field-free zone of the mass spectrometer with the cluster beam. A parent cluster with mass m_P and laboratory kinetic energy E_{Lab} will form by collision-induced dissociation, fragments with mass m_F and kinetic energy $E_F = (m_F/m_P)E_{Lab}$. An electrical voltage applied on a grid, placed in front of the MCP detector, rejects all of the fragments that have kinetic energy lower than the voltage. By scanning this voltage, the energy of the fragments is measured and used to derive their molecular mass, hence identifying the fragmentation channels of the parent cluster. The rejection of all fragments allows the measurement of fragmentation degree and can be used to obtain the fragmentation cross sections (see section 3.2).

2.2. DFT Calculations. The theoretical calculations were performed at the B3LYP[21−23] level of approximation within the DFT and the LANL2DZ basis set as implemented in the Gaussian 03 program.[24] We calculate the gas-phase Gibbs free energy of formation (T = 298.15 K, P = 1 atm) of the iron oxide clusters from the expression $\Delta G_{formation} = G_{products} - G_{reactants}$. The total free energy (G) of each system is the sum of the electronic and thermal free-energy corrections, including contributions from vibrational, rotational, and translational motions. All of the systems were fully relaxed without any symmetry constraints. Vibrational frequencies were calculated for all of the optimized systems, and real frequencies were obtained in all cases. All possible spin states were taken into consideration for every different complex.

3. RESULTS AND DISCUSSION

3.1. Laser Ablation Experiments: Formation and Stability of Clusters. In Figure 1, we present two typical mass spectra of the cationic iron oxide complexes obtained by laser ablation using (a) UV (266 nm) and (b) IR (1064 nm) laser ablation of Fe in an O_2 molecular beam, showing the formation of mainly FeO_n^+ clusters. Water impurities present in the gas inlet system led to the formation of hydrated clusters (marked by triangles in Figure 1), with the general formula $FeO_n(H_2O)^+$ (n = 2, 4, 6, 8). Small amounts of $Fe_2O_n^+$ (n = 2−5) clusters were also detected (Figure 1b).

The laser ablation of a metallic target leads to the ejection of mainly atoms in neutral or ionic form. The clusters are formed exclusively by collisions in the mixing region of the ablation plume with the O_2 molecular beam. Therefore, the source used here (open configuration) produces clusters of the type MX_n (M = ablated metal atom; X = atomic or molecular gas).[18,20,25] This is the cause for the preferential formation of the oxygen-rich monoiron FeO_n^+ species in our case, different from other experiments[2−10] in which Fe_mO_n ($m \geq 1$) complexes are formed through multiple collisions in a cluster growth channel.

The main characteristic of the FeO_n^+ clusters series (up to n = 10) is that complexes with an even number of oxygen atoms have a higher abundance compared to those with an odd number of O atoms. This behavior has been also observed in the spectra

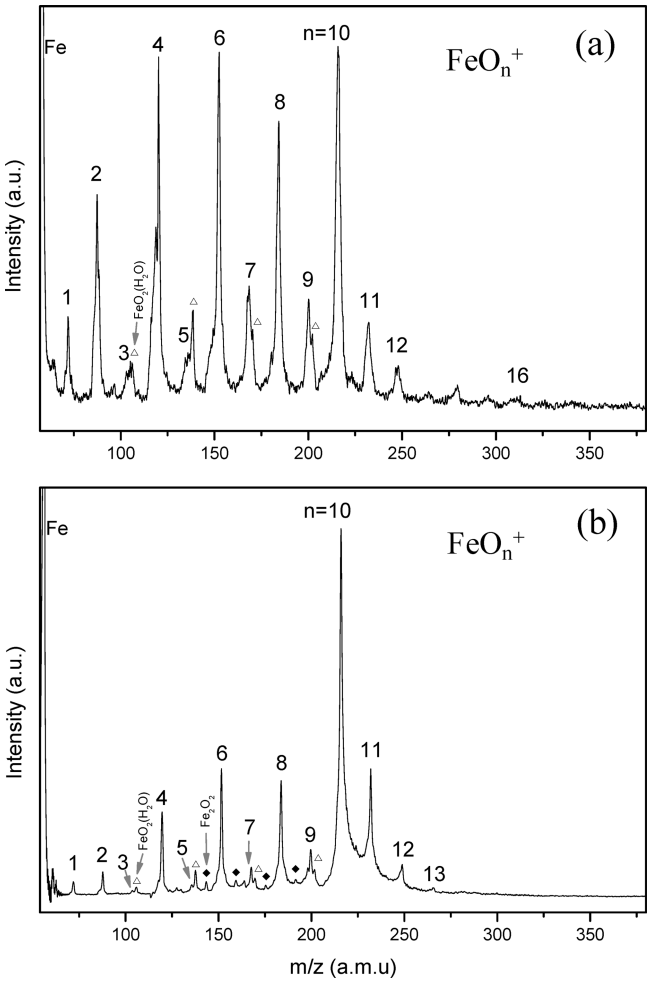

Figure 1. Mass spectra of iron oxide clusters obtained by (a) UV and (b) IR laser ablation and 4 times higher O_2 flow rate. The △ indicate the hydrated clusters (see text), and the ◆ show the position of Fe_2O_n clusters.

of Reilly et al.,[4] where an odd−even intensity alternation up to FeO_9^+ is evident in the mass spectrum presented.

Another interesting feature in Figure 1 is the relative high intensity of FeO_{10}^+, followed by a sharp decrease in intensity for clusters with more than 10 oxygen atoms. A similar trend (odd−even alternation and high intensity of the cluster containing 10 O atoms) was observed in our experiments for other systems (NbO_n, TaO_n)[26] and was also reported (without further comment) by other groups for Nb- and Ta-oxide clusters.[27−29]

It should be noticed that the signal at m/z = 216 could be attributed either to FeO_{10}^+ (main isotopic peak at m/z = 215.88) or to $Fe_3O_3^+$ (m/z = 215.79). Although the mass resolution of our apparatus for these experiments does not allow an unambiguous assignment through the separation of the two possible signals or through isotopic ratio measurement, we attribute this peak to the FeO_{10}^+ cluster because the formation of $Fe_3O_3^+$ is highly improbable in our experimental conditions, as explained bellow.

Larger clusters, $Fe_{m>1}O_n^+$, would be formed via gas-phase association reactions[30] for which FeO^+ formation by the $Fe^+ + O_2 \rightarrow FeO^+ + O$ reaction is the initial step. This reaction is known to be highly endothermic (see section 3.3 and ref 31) and

has a negligible (~0.05 Å^2) cross section at thermal collision energies;[31] therefore, it is not expected to occur in our experiment. Moreover, a large number of (three-body) collisions is needed for the formation of $Fe_{2,3,4,...}O_n^+$ clusters. This is generally achieved[2−10] by the use of "closed" cluster sources where the mixing of the laser-formed plasma with the ligand gas occurs in a confined space (cluster growth channel). This situation has been nicely investigated by Reilly et al.,[4] proving that an increase by a factor of ~2 of the growth channel (conical expansion nozzle) length was needed in order to produce $Fe_2O_n^+$ clusters. Under such conditions, in an "open" cluster source, the intensity of the $Fe_{m>1}O_n$ drops rapidly as the number of Fe atoms (m) increases. As a result, the amount of $Fe_{3,4,...}O_n$ is expected to be much lower than that of Fe_2O_n and in the present case vanishing.

3.2. Crossed Molecular Beam Experiments: Fragmentation of Clusters. Besides the mass spectrometric work, the stability of $Fe(O_2)_n^+$ clusters has been investigated experimentally with a different approach, based on collisional fragmentation of the produced clusters by noble gas (Ne) atom impact and fragment separation. The measurement of fragments' masses (see section 2.1) indicates that the clusters dissociate by successive loss of O_2, in good agreement with the results of Reilly et al.[4] for collision-induced dissociation of FeO_n^+ clusters with Xe. The loss of O_2 in the case of the peak at m/z = 216 confirms its assignment as $Fe(O_2)_5^+$. The $Fe_3O_3^+$, which has the same mass, exhibits different fragmentation channels, with the loss of FeO, FeO_2, and Fe_2O_3, as earlier photofragmentation experiments of Molek et al.[5] had shown.

The fragments' rejection (by applying a potential barrier on the grid placed before the MCP) results in an intensity attenuation of the parent cluster beam. The application of the Beer's law $I_r = I_0 \cdot \exp(-QNL)$ allows the measurement of the fragmentation cross section Q from the reduced intensity I_r of a given parent cluster, its initial intensity I_0, the number density N of the target gas, and the length L of the crossing region of the two beams. The last two parameters are not known but are common for all of the clusters, thus allowing the relative comparison of the individual cross sections. TOF spectra are recorded with the secondary Ne beam on and off in order to account for possible metastable fragmentation and/or fragmentation due to the background gas.

The so-obtained cross sections are plotted in Figure 2 (black squares) with some indicative error bars due mainly to reproducibility of the data.

Li et al.[8] performed experimental studies on the kinetic energy dependence of collision-induced dissociation on mass selected $Fe_mO_n^+$ (m = 1−3, n = 1−6) with Xe. They measured the thermochemistry and the fragmentation cross sections for FeO_2^+ and FeO_4^+. The cross section values for a center-of-mass collision energy of around 15 eV, including all possible fragmentation channels, are ~11 Å^2 for FeO_2^+ + Xe and ~19 Å^2 for FeO_4^+ + Xe[8] and are displayed in Figure 2 (gray circles). By normalizing our data to the first value, a very good agreement is achieved for FeO_4^+, despite the two totally different experimental methods involving different collision gases and collision energies.

The fragmentation cross section provides direct evidence for the relative stability of the clusters. The lower value (dip) for FeO_{10}^+ in Figure 2 reflects the special stability of this complex and supports the results from the mass spectra discussed in the previous section. A detailed presentation of the fragmentation method and the analysis of the obtained results will be presented in a forthcoming paper.

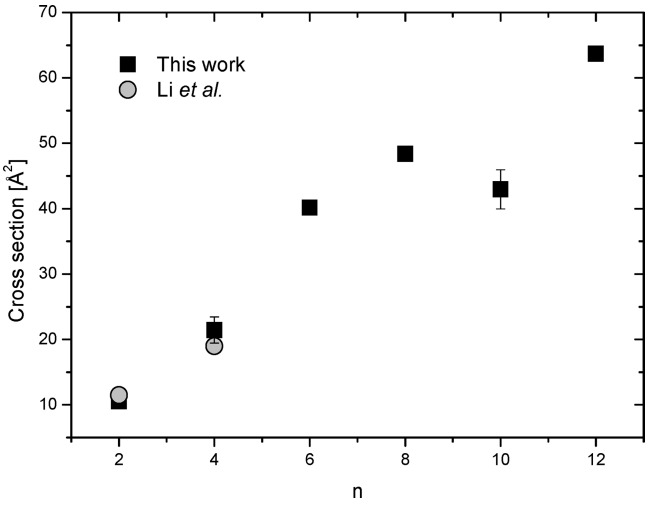

Figure 2. Fragmentation cross sections of FeO_n^+ clusters as a function of the cluster size n in collisions with Ne (this experiment, solid squares) and Xe (Li et al., ref 8, gray circles).

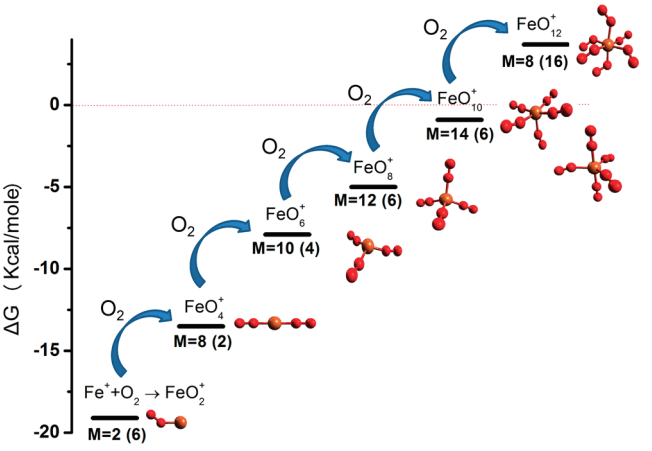

Figure 3. Variation of the Gibbs free energy for the reactions $FeO_{2n}^+ + O_2 \rightarrow FeO_{2(n+1)}^+$, n = 0−5. Structures corresponding to the ground state are also shown.

3.3. DFT Calculations: Growth Mechanism of Clusters. To explain the mass spectra and unravel the structural characteristics of the complexes, we now turn to computations by first principles. In Figure 3, we present the free energy of formation (ΔG) of various positively charged iron oxide clusters with an even number of O atoms (six reaction steps leading to the formation of FeO_{12}^+). ΔG for FeO_{2n}^+ is defined with respect to the reactions $FeO_{2n}^+ + O_2 \rightarrow FeO_{2(n+1)}^+$, n = 0−5. M denotes the multiplicity of the ground state, whereas the numbers in parentheses indicate the multiplicity of the structures that are almost isoenergetic to the ground states ($\Delta E \leq 2$ kcal/mol). For example, the FeO_{10}^+ system exhibits two isoenergetic ground states, one of multiplicity 6 and the other of multiplicity 14.

Figure 3 clearly shows that as the number of O_2 molecules attached to the Fe cation increases, the reactions become gradually less exothermic, with the last thermodynamically driven formed cluster being the FeO_{10}^+. The formation of larger

clusters (i.e., FeO_{12}^+) becomes endothermic. Similar calculations were performed for clusters with an odd number of O atoms (results not shown here). In this case, the initial reaction associated with the formation of the clusters is $Fe^+ + O_2 \rightarrow FeO^+ + O$. However, this reaction (dissociation of O_2 in the presence of Fe^+) was found to be highly endothermic (ΔG = +26.4 kcal/mol). As a result, the formation of clusters with an odd number of O atoms is not thermodynamically favored. These observations suggest that the formation of FeO_{2n}^+ clusters, with $n = 1-5$, is favored, in agreement with the experimental data. In addition, they justify the relative intensities in the mass spectra shown in Figure 1, considering that the reactions take place in the atmosphere of O_2 molecules, in which the presence of atomic oxygen is limited. All clusters presented in Figure 3 are very stable, as shown in Table 1S of the Supporting Information.

The fully optimized ground-state geometries are presented as inset pictures in Figure 3. By investigating all possible spin multiplicities, we found no signs of molecular O_2 dissociation compared to neutral and negatively charged clusters.[15] It is worth noticing in Figure 3 the systematic appearance of almost isoenergetic high-spin (HS) and low-spin (LS) ground states, which do not exhibit any noticeable structural differences, for these subnanometer clusters. This was also found in our earlier studies of small Fe−Co clusters.[32] Other systems presenting the LS−HS ground states as well are the bulk Fe_2O_3,[33] the bulk binaries consisting of any pairs of Fe, Co, Ni, Cu,[34] the tetrahedrally bonded magnetic III-nitride semiconductors doped with transition metals,[35] and so forth.

In addition to the thermodynamics information, Figure 3 describes the evolution of FeO_n^+ clusters' structural characteristics during their growth. It is observed that the linear geometry of FeO_2^+ and FeO_4^+ turns into oblique tetrahedral (T_d) for FeO_6^+ and becomes a rather regular tetrahedron for $n = 8$. For $n = 10$ and 12, we observe the clusters' tendency to recover the octahedral (O_h) structure (with a competitive trigonal bipyramidal structure for $n = 10$). In view of these observations, one can argue that the number of the O_2 ligands attached (bonded) to the Fe cation dictates the local point group symmetry of the Fe ion, which in turn is depicted in the directional preferences of the hybridized d orbitals. This can explain the structural changes observed up to FeO_{10}^+. The FeO_{10}^+ exhibits two isoenergetic ground-state structures (ΔE = 0.3 kcal/mol). One is closer to the octahedral structure (stabilized in multiplicities 6 and 14), whereas the other has tetrahedral characteristics (trigonal bipyramid, stabilized in multiplicity 14). That is, FeO_{10}^+ appears to be a turn-point transition structure between the tetrahedral (FeO_8^+) and the octahedral symmetry (FeO_{12}^+) for the FeO_{2n}^+ series.

Besides the thermodynamics favoring the formation of the FeO_{10}^+ complex, we further investigated if there are any kinetic reasons preventing the formation of the FeO_{12}^+ cluster from FeO_{10}^+. For this purpose, we selected the O_h ground-state structure of FeO_{10}^+, in which Fe^+ is accessible to the approach of an O_2 molecule (in the T_d structure, Fe^+ is fully protected by the O_2 ligands). In addition, this structure leads to the formation of the octahedrally coordinated FeO_{12}^+. The potential energy surface scan of the reaction $FeO_{10}^+ + O_2 \rightarrow FeO_{12}^+$ presented in Figure 4, for both HS and LS states, shows the absence of any kinetic barrier. This is the reason why the thermodynamic picture predicted by our calculations lies in perfect agreement with the experiments. The formation of this series of complexes is thermodynamically driven.

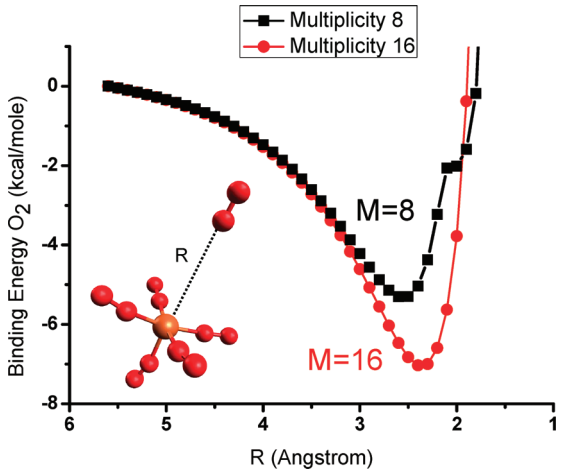

Figure 4. Barrierless potential energy surface scan of the O_2 interaction with FeO_{10}^+, leading to the formation of FeO_{12}^+ in both HS and LS states.

3.4. Magnetic Properties of Clusters. The magnetic characteristics of the iron oxide clusters exhibit unique behavior. As the cluster size n increases, the magnetic moment of the FeO_{2n}^+ clusters also increases. As stated above, for each size, there are always two low-energy structures, one with HS and one with LS. We found that in the HS state, the magnetic moments of all O_2 ligands are aligned parallel to the magnetic moment of Fe^+, leading to ferromagnetic coupling. On the other hand, in the LS state, the magnetic moments of the O_2 ligands are aligned antiferromagnetically to that of Fe^+. Considering that each O_2 contributes two unpaired electrons, in the HS state of FeO_{2n} ($n = 1 - 6$) clusters, the magnetic moment of the Fe cation is 3 μB. It is worth noticing that, in view of these results, the directional flipping of the magnetic moment of the Fe^+ takes place without any energy cost. The multiplicities of the LS state of FeO_{2n} ($n = 1-4$) clusters can be attributed to the flipping of the magnetic moment of Fe^+ (−3 μB). This however does not seem to be the case for FeO_{10}^+ and FeO_{12}^+, where the LS multiplicities were found to be 6 and 8 instead of 8 and 10, respectively. The decline of these clusters from the simple Fe flipping explanation can be justified by their structural changes. As already discussed, the FeO_{2n}^+ clusters with $n \geq 5$ adopt an octahedral symmetry instead of the tetrahedral one adopted by the smaller clusters. In fact, we found that the T_d symmetry cannot be stabilized in the LS state of FeO_{10}^+ (cluster relaxes to the O_h structure), whereas it can be stabilized in the HS state. As a result of this symmetry change, the Fe(3d) orbitals become rehybridized, leading to a larger crystal field splitting for the O_h symmetry in the LS state and a repopulation of the d orbitals accordingly. In the HS states, both O_h and T_d structures of FeO_{10}^+ are stabilized, indicating that any changes due to the crystal field splitting are counterbalanced by the difference in the exchange interaction between the Fe^+ and the O_2 ligands. By combining the experimental and theoretical information, we conclude that the thermodynamically favored complex, showing the highest magnetic moment, is the FeO_{10}^+. This molecular cluster has approximately a 0.5 nm diameter and can accommodate in its orbitals 13 unpaired electrons. It is worth noting that the HS−LS behavior is observed on the neutral cluster as well (see Figure 1S of the Supporting Information file).

4. CONCLUSIONS

Summarizing, in this work, we systematically investigated the FeO_n^+ clusters by both experiments and first-principle calculations. The results indicate that the largest thermodynamically stable complex is FeO_{10}^+, which additionally is characterized by a symmetry transition from tetrahedral to octahedral structure. All of the FeO_{2n}^+ clusters exhibit isoenergetic HS and LS states due to the magnetic moment flipping on Fe^+. As a result, the FeO_{10}^+ has two isoenergetic ground states of multiplicities 14 (HS) and 6 (LS). Both experiments and calculations show the thermodynamic preference for the formation of clusters with an even number of oxygen atoms. Finally, this study provides property-driven directions for materials design. Sorbent materials with accessible metal sites (cationic Fe) can attract O_2 molecules and form stable complexes with tunable magnetic domains.

■ ASSOCIATED CONTENT

Supporting Information. Table with the stability of the FeO_{2n}^+ complexes and graph showing the HS−LS behavior of the neutral FeO_{10} cluster. This material is available free of charge via the Internet at http://pubs.acs.org.

■ AUTHOR INFORMATION

Corresponding Author
*E-mail: vele@iesl.forth.gr.

■ ACKNOWLEDGMENT

G.M. is supported by a Marie Curie International Outgoing Fellowship within the seventh European Community Framework Programme. The authors would like to thank J. Labrakis for his helpful assistance in the experimental work.

■ REFERENCES

(1) Palotas, K.; Andriotis, A. N.; Lappas, A. *Phys. Rev. B* **2010**, *81*, 075403.
(2) Wang, L.-S.; Wu, H.; Desai, S. R. *Phys. Rev. Lett.* **1996**, *76*, 4853.
(3) Wang, Q.; Sun, Q.; Sakurai, M.; Yu, J. Z.; Gu, B. L.; Sumiyama, K.; Kawazoe, Y. *Phys. Rev. B* **1999**, *59*, 12672.
(4) Reilly, N. M.; Reveles, J. U.; Johnson, G. E.; del Campo, J. M.; Khanna, S. N.; Köster, A. M.; Castleman, A. W. *J. Phys. Chem. C* **2007**, *111*, 19086.
(5) Molek, K. S.; Anfuso-Cleary, C.; Duncan, M. A. *J. Phys. Chem. A* **2008**, *112*, 9238.
(6) Xie, Y.; Dong, F.; Heinbuch, S.; Rocca, J. J.; Bernstein, E. R. *J. Chem. Phys.* **2009**, *130*, 114306.
(7) Yin, S.; Xue, W.; Ding, X.-L.; Wang, W.-G.; He, S.-G.; Ge, M.-F. *Int. J. Mass Spectrom.* **2009**, *281*, 72.
(8) Li, M.; Liu, S.-R.; Armentrout, P. B. *J. Chem. Phys.* **2009**, *131*, 144310.
(9) Schröder, D.; Fiedler, A.; Schwarz, J.; Schwarz, H. *Inorg. Chem.* **1994**, *33*, 5094.
(10) Xue, W.; Yin, S.; Ding, X.-L.; He, S.-G.; Ge, M.-F. *J. Phys. Chem. A* **2009**, *113*, 5302.
(11) Atanasov, M. *Inorg. Chem.* **1999**, *38*, 4942.
(12) Gutsev, G. L.; Khanna, S. N.; Rao, B. K.; Jena, P. *J. Phys. Chem. A* **1999**, *103*, 5812.
(13) Lopez, S.; Romero, A. H.; Mejia-Lopez, J.; Mazo-Zuluaga, J.; Restrepo, J. *Phys. Rev. B* **2009**, *80*, 085107.
(14) Shiroishi, H.; Oda, T.; Hamada, I.; Fujima, N. *Eur. Phys. J. D* **2003**, *24*, 85.
(15) Gutsev, G. L.; Weatherford, C. A.; Pradhan, K.; Jena, P. *J. Phys. Chem. A* **2010**, *114*, 9014.
(16) Glukhovtsev, M. N.; Bach, R. D.; Nagel, C. J. *J. Phys. Chem. A* **1997**, *101*, 316.
(17) Lüder, C.; Georgiou, E.; Velegrakis, M. *Int. J. Mass Spectrom. Ion Processes* **1996**, *153*, 129.
(18) Prekas, D.; Lüder, C.; Velegrakis, M. *J. Chem. Phys.* **1998**, *108*, 4450.
(19) Velegrakis, M.; Sfounis, A. *Appl. Phys. A* **2009**, *97*, 765.
(20) Velegrakis, M. In *Advances in Metal and Semiconductor Clusters*; Duncan, M. A., Ed.; JAI Press: London, 2001; Vol. IX.
(21) Becke, A. D. *Phys. Rev. A* **1988**, *38*, 3098.
(22) Becke, A. D. *J. Chem. Phys.* **1993**, *98*, 5648.
(23) Lee, C. T.; Yang, W. T.; Parr, R. G. *Phys. Rev. B* **1988**, *37*, 785.
(24) Frisch, M. J.; Trucks, G. W.; Schlegel, H. B.; Scuseria, G. E.; Robb, M. A.; Cheeseman, J. R.; Montgomery, J. A., Jr.; Vreven, T.; Kudin, K. N.; Burant, J. C.; Millam, J. M.; Iyengar, S. S.; Tomasi, J.; Barone, V.; Mennucci, B.; Cossi, M.; Scalmani, G.; Rega, N.; Petersson, G. A.; Nakatsuji, H.; Hada, M.; Ehara, M.; Toyota, K.; Fukuda, R.; Hasegawa, J.; Ishida, M.; Nakajima, T.; Honda, Y.; Kitao, O.; Nakai, H.; Klene, M.; Li, X.; Knox, J. E.; Hratchian, H. P.; Cross, J. B.; Bakken, V.; Adamo, C.; Jaramillo, J.; Gomperts, R.; Stratmann, R. E.; Yazyev, O.; Austin, A. J.; Cammi, R.; Pomelli, C.; Ochterski, J. W.; Ayala, P. Y.; Morokuma, K.; Voth, G. A.; Salvador, P.; Dannenberg, J. J.; Zakrzewski, V. G.; Dapprich, S.; Daniels, A. D.; Strain, M. C.; Farkas, O.; Malick, D. K.; Rabuck, A. D.; Raghavachari, K.; Foresman, J. B.; Ortiz, J. V.; Cui, Q.; Baboul, A. G.; Clifford, S.; Cioslowski, J.; Stefanov, B. B.; Liu, G.; Liashenko, A.; Piskorz, P.; Komaromi, I.; Martin, R. L.; Fox, D. J.; Keith, T.; Al-Laham, M. A.; Peng, C. Y.; Nanayakkara, A.; Challacombe, M.; Gill, P. M. W.; Johnson, B.; Chen, W.; Wong, M. W.; Gonzalez, C.; Pople, J. A. *Gaussian 03*, revision D.01; Gaussian, Inc.: Wallingford, CT, 2004.
(25) Lüder, C.; Prekas, D.; Velegrakis, M. *Laser Chem.* **1992**, *17*, 109.
(26) Mihesan, C.; Jadraque, M.; Velegrakis, M.; in preparation.
(27) Zemski, K. A.; Justes, D. R.; Castleman, A. W. *J. Phys. Chem. B* **2002**, *106*, 6136.
(28) Zemski, K. A.; Bell, R. C.; Castleman, A. W., Jr. *Int. J. Mass Spectrom.* **1999**, *184*, 119.
(29) Molek, K. S.; Jaeger, T. D.; Duncan, M. A. *J. Chem. Phys.* **2005**, *123*, 144313.
(30) Guo, B. C.; Kerns, K. P.; Castleman, A. W. *Int. J. Mass Spectrom. Ion Processes* **1992**, *117*, 129.
(31) Fisher, E. R.; Elkind, J. L.; Clemmer, D. E.; Georgiadis, R.; Loh, S. K.; Aristov, N.; Sunderlin, L. S.; Armentrout, P. B. *J. Chem. Phys.* **1990**, *93*, 2676.
(32) Mpourmpakis, G.; Froudakis, G. E.; Andriotis, A. N.; Menon, M. *Phys. Rev. B* **2005**, *72*, 104417.
(33) Bhanu Ghosh, D.; de Gironcoli, S. Structural and spin transitions in Fe_2O_3. In eprint arXiv:0903.2104, 2009; Vol. [cond-mat.mtrl-sci].
(34) James, P.; Eriksson, O.; Johansson, B.; Abrikosov, I. A. *Phys. Rev. B* **1999**, *59*, 419.
(35) Cui, X. Y.; Delley, B.; Freeman, A. J.; Stampfl, C. *Phys. Rev. Lett.* **2006**, *97*, 016402.